Targeting antigen to bone marrow stromal cell-2 expressed by conventional and plasmacytoid dendritic cells elicits efficient antigen presentation

Jessica M. Moffat[1,2], Elodie Segura[3,4], Gabriela Khoury[5,6], Irene Caminschi[1,7], Paul U. Cameron[6,8,9], Sharon R. Lewin[6,8,9], Jose A. Villadangos[1,2,10] and Justine D. Mintern[1,10]

[1] Walter and Eliza Hall Institute, Parkville, Victoria, Australia
[2] Department of Microbiology and Immunology, The University of Melbourne, Parkville, Victoria, Australia
[3] Institut National de la Sante et de la Recherche Medicale Unite 932, Paris, France
[4] Center de Recherche, Institut Curie, Paris, France
[5] Department of Medicine, Monash University, Victoria, Australia
[6] Centre for Virology, Burnet Institute, Prahran, Victoria, Australia
[7] Center for Immunology, Burnet Institute, Prahran, Victoria, Australia
[8] Department of Infectious Diseases, Monash University, Victoria, Australia
[9] Infectious Diseases Unit, Alfred Hospital, Prahran, Victoria, Australia
[10] Department of Biochemistry and Molecular Biology, The University of Melbourne, Parkville, Victoria, Australia

Bone marrow stromal cell-2 (BST-2) has major roles in viral tethering and modulation of interferon production. Here we investigate BST-2 as a receptor for the delivery of antigen to dendritic cells (DCs). We show that BST-2 is expressed by a panel of mouse and human DC subsets, particularly under inflammatory conditions. The outcome of delivering antigen to BST-2 expressed by steady state and activated plasmacytoid DC (pDC) or conventional CD8$^+$ and CD8$^-$ DCs was determined. T-cell responses were measured for both MHC class I (MHCI) and MHC class II (MHCII) antigen presentation pathways in vitro. Delivering antigen via BST-2 was compared with that via receptors DEC205 or Siglec-H. We show that despite a higher antigen load and faster receptor internalisation, when antigen is delivered to steady state or activated pDC via BST-2, BST-2-targeted activated conventional DCs present antigen more efficiently. Relative to DEC205, BST-2 was inferior in its capacity to deliver antigen to the MHCI cross-presentation pathway. In contrast, BST-2 was superior to Siglec-H at initiating either MHCI or MHCII antigen presentation. In summary, BST-2 is a useful receptor to target with antigen, given its broad expression pattern and ability to access both MHCI and MHCII presentation pathways with relative efficiency.

Additional supporting information may be found in the online version of this article at the publisher's web-site

Correspondence: Dr. Justine D. Mintern
e-mail: jmintern@unimelb.edu.au

Introduction

Bone marrow stromal cell antigen-2 (BST-2; also CD317, PDCA-1, tetherin and HM1.24) is a widely utilised plasmacytoid dendritic cell (pDC) marker due to its high expression by pDCs in steady state mouse model systems [1]. BST-2 is an interesting molecule with unusual topology in that it contains a large extracellular domain, a cytoplasmic N-terminus and a C-terminus that is GPI-anchored in the plasma membrane [2]. Major functions for BST-2 include modulation of pDC interferon (IFN)-α production [1, 3] and the tethering of newly formed enveloped viral particles to the infected cell surface [4]. BST-2 virus tethering capacity was first described for HIV [4] and is now considered to occur for many, if not all, enveloped viruses [5]. Here we speculate that BST-2 tethering facilitates pDC antigen presentation. A major role for pDCs in efficient antigen presentation, particularly relative to conventional DCs (cDCs) is controversial [6], however, it is generally accepted that pDCs, particularly following activation, have the capacity to present antigen via MHC class I (MHCI) and MHC class II (MHCII) [7]. BST-2 may act as a receptor that confers anti-viral antigen presentation properties to pDCs, given the high expression of BST-2 by this cell type. In support of this hypothesis is the observation that BST-2 can be utilised as a target molecule for antigen delivery in vivo [8–10] and can modulate CD8$^+$ T-cell priming to viral antigen [11].

Incorporating antigen into a monoclonal antibody to target specific DC surface markers is an effective strategy for eliciting protective (and tolerising) immune responses [12]. A number of DC surface molecules have been targeted to date, including BST-2. Administration of BST-2-targeted ovalbumin (OVA) in vivo elicits antigen presentation [8–10] and importantly can initiate immunity that is capable of protecting mice from vaccinia virus-OVA and reducing tumour growth following implantation of B16-OVA melanoma [9]. In these studies, BST-2 targeting in vivo was undertaken utilising an adjuvant regime that ensured BST-2 presentation was restricted to pDCs, with the role of cDCs excluded [8–10]. Here we will evaluate the outcomes of targeting BST-2 by a broader panel of DC subsets in order to evaluate its efficiency as an antigen receptor by DC, including both CD8$^+$ and CD8$^-$ DCs that have the capacity to express it under specific conditions. Translating antibody-mediated targeting of DC molecules into settings of vaccination against human disease is the obvious next step. Vaccines based on DC targeting are currently being evaluated by Celldex Therapeutics in PhaseI/II clinical trials for the treatment of solid cancers. DEC205 is the focus of several clinical studies. How would this strategy fare for human BST-2? BST-2 is already a target for antibody-induced cytotoxicity as an immunotherapy to eliminate tumours [13, 14]. Utilising anti-BST-2 to target antigen for vaccine-mediated immunotherapy relies on BST-2 expression by human DC subsets. Previous studies suggest BST-2 is expressed at low levels by human peripheral blood pDCs, but can be up-regulated by activation [3,15]. Here we will analyse BST-2 expression by a panel of human DC subsets.

While there is a growing list of molecules that can act as recipients for targeted antigen, the relative efficiency of unique DC receptors that are expressed by different DC subsets is mostly unknown. Factors that will impact the outcome of DC targeting include the specific DC subset that is targeted, its activation status, the amount of antigen delivered (antigen load), the rate of receptor internalisation and the trafficking route accessed by the targeted molecule. In one study, a direct comparison of targeting BST-2 to Siglec-H showed that while targeting BST-2 elicited a robust antibody response, targeting Siglec-H did not [10]. This is a pertinent example of the divergent outcomes that can result from targeting distinct DC markers. The underlying mechanisms that determine the outcome of antigen delivery are of interest if this strategy is to be effectively utilised therapeutically. Here we have investigated BST-2 in the context of antigen delivery and examined the efficiency of BST-2 targeting, relative to DEC205 and Siglec-H by delivering antigen to defined DC subsets, including both pDCs and cDCs. Evaluating BST-2 targeting outcomes by a panel of different DC subsets has not been previously examined. The ability of BST-2 to facilitate MHCI and MHCII antigen presentation by steady state and activated CD8$^+$ DCs, CD8$^-$ DCs and pDCs and the underlying factors that contribute to the presentation of delivered antigen were determined.

Results

Expression profile of BST-2 transcription and surface protein by mouse immune cells

BST-2 expression for a panel of immune cells, including pDCs (CD11c^{int} Ly6c$^+$), CD8$^+$ DCs (CD11c$^+$ CD8$^+$), CD8$^-$ DCs (CD11c$^+$ CD8$^-$), macrophages (CD11b$^+$ F480$^+$), B (B220$^+$ CD19$^+$) and T lymphocytes (CD3$^+$), was analysed by quantitative real-time PCR to assess *BST-2* transcription. To assess *BST-2* transcription, cells were analysed immediately following isolation (steady state) or following treatment with specific stimuli to elicit activation (in vitro activated). Analysis of the steady state samples showed mouse spleen pDCs expressed the highest level of *BST-2* mRNA. Following in vitro activation, all of the immune cell types, with the exception of B cells, increased *BST-2* transcription (Fig. 1A).

BST-2 cell surface protein expression was monitored by flow cytometry for a similar panel of immune cells. In this case, cell activation was achieved either by stimulating with cell specific stimuli as performed for the transcriptional analysis (Fig. 1B) or following isolation of cells from mice that had received nonmethylated cytosine-guanosine oligonucleotides (CpG) intravenously as an inflammatory stimulus in vivo (Fig. 1C). At steady state, pDCs express high levels of surface BST-2, while other immune cell types express it low levels. Following in vitro activation with cell specific stimuli, cDCs, macrophages, B cells and T cells all up-regulate BST-2 surface expression. Interestingly, activation via the T-cell receptor increased BST-2 expression by T cells (Fig. 1B). BST-2 surface expression was also elevated on all immune cell subsets isolated 24 h following in vivo CpG administration (Fig. 1C) and on DC subsets isolated from the lung parenchyma of mice infected with influenza A virus three days previously (Fig. 1D).
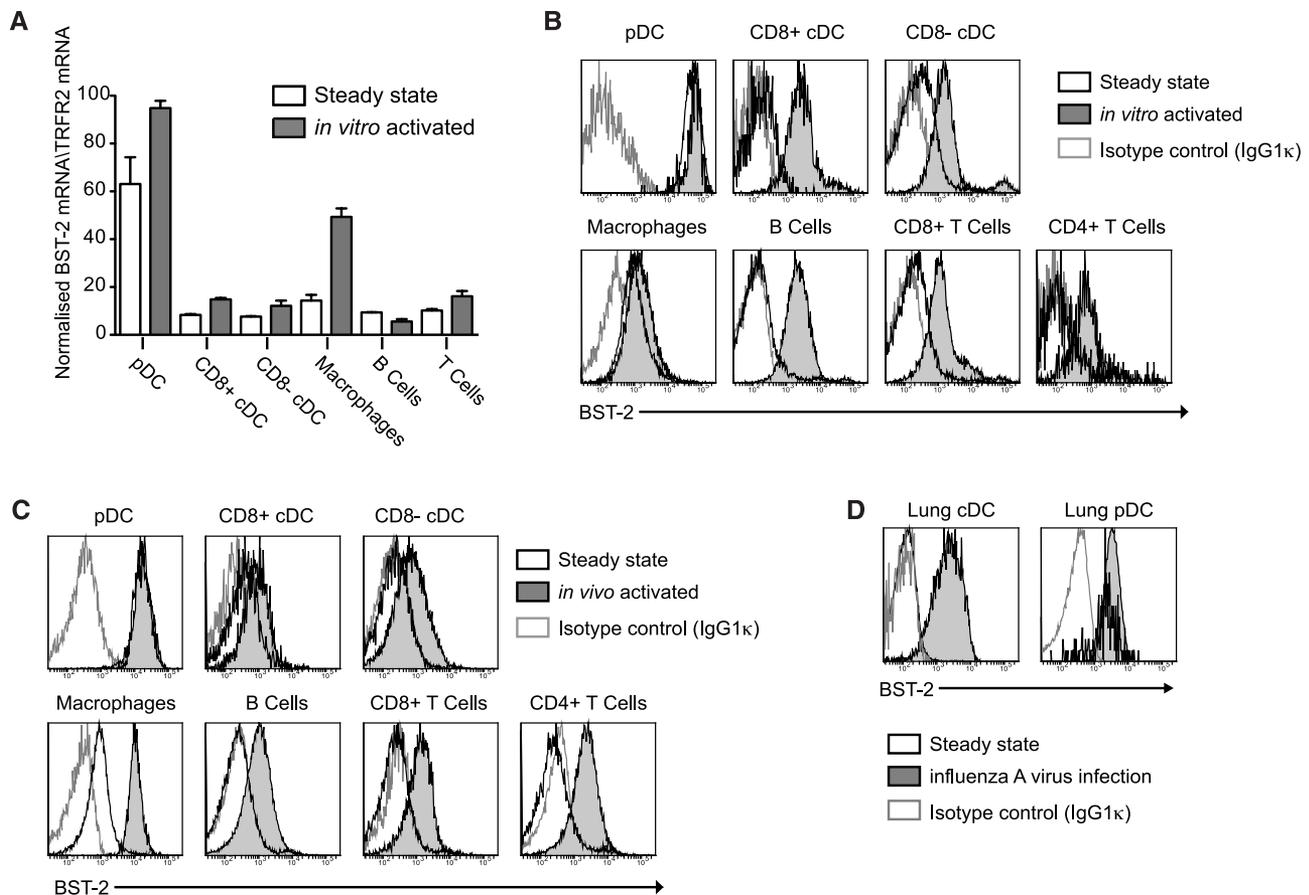
Figure 1. Expression profiles of BST-2 transcription and surface protein by mouse immune cells. (A) mRNA was isolated from sorted steady state or in vitro CpG-activated pDCs, CpG-activated CD8^{+} DCs, CpG-activated CD8^{−} DCs, anti-CD40-activated B cells, anti-CD3, anti-CD28 and IL-2-activated T cells and IFN-γ and LPS-activated peritoneal macrophages. The level of BST-2 mRNA expression relative to house-keeping gene transferin receptor 2 was determined by quantitative real time PCR. Data are shown as mean + SEM of four samples pooled from two independent experiments. (B) Surface protein expression of BST-2 was assessed by flow cytometry for the same panel of cells as described in (A). The data are representative of two individual experiments, with three mice analysed per experiment. (C) Surface protein expression of BST-2 was assessed by flow cytometry for cells isolated from steady state mice or mice that had received CpG 24 h previously. The data are representative of three individual experiments, with three mice analysed per experiment. (D) Surface protein expression of BST-2 for pDCs and cDCs isolated from lungs of mice infected three days previously with influenza A virus. The data are representative of two independent experiments, with three mice pooled per sample.

Expression profile of BST-2 transcription and surface protein by human DCs

Human DC subsets were probed for BST-2 expression. First, we undertook a transcriptional microarray analysis of BST-2 by a panel of human DC including immature and mature monocyte-derived DCs, blood CD1c^{+} myeloid DCs (mDCs), blood pDCs, skin CD14^{+} dermal DCs, CD1a^{+} dermal DCs and epidermal Langerhans cells. Expression of BST-2 mRNA was also assessed for inactivated and activated T cells. All human DC subsets displayed high levels of BST-2 transcription. Monocyte-derived DCs did not up-regulate BST-2 following activation with TNF-α, whereas an obvious increase in BST-2 transcription was detected following activation of T cells (Fig. 2A).

To evaluate cell surface BST-2 protein expression by human DCs and monocytes, we examined BST-2 expression by flow cytometry for CD14 monocytes, CD16 monocytes, BDCA1 mDCs,

Clec9A mDCs and pDCs isolated from blood. DCs were examined directly following isolation and following activation with R848, a TLR7/8 ligand that stimulates all the isolated subsets. Interestingly, in direct contrast to murine DC, low levels of BST-2 were expressed by pDCs at steady state (inactivated) in contrast to the other subsets examined. Inactivated Clec9A mDCs expressed high BST-2 levels as did CD14 monocytes. R848 activation increased BST-2 expression by both the monocytes and DCs, with the exception of the Clec9A mDCs that remained BST-2^{high} (Fig. 2B). Therefore, BST-2 exhibits a unique pattern of expression by human DCs, relative to murine DCs.

Antigen load, receptor internalisation and antigen-presentation efficiency of targeted DC subsets

BST-2 has been previously targeted with antigen to elicit T-cell immunity in vivo [8–10]. Here we dissected antigen-presentation
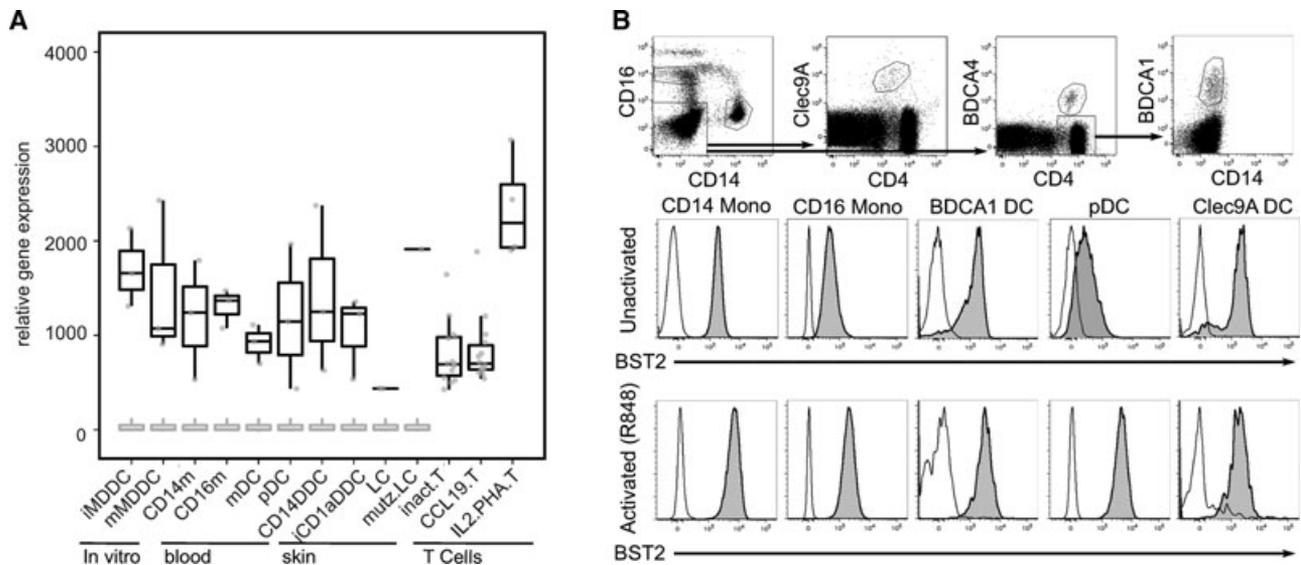
Figure 2. Expression profiles of BST-2 transcription and surface protein by human dendritic cells. (A) The relative expression of *BST-2* mRNA is shown for immature monocyte-derived DC or mature monocyte-derived DCs, peripheral blood myeloid DCs (mDC) or plasmacytoid DCs (pDC), skin CD14^{+} dermal DCs (CD14DDC), CD1a^{+} dermal DCs (CD1aDDC), Langerhans cells (LC) or mutz. LC generated from the MUTZ3 cell line, inactivated T cells (inact. T), CCL19-stimulated T cells (CCL19.T) or IL-2, PHA-stimulated T cells (IL2.PHA.T). A box plot for *BST-2* is shown compared with unselected gene expression for the same population. Data are shown as dot plot and box plot with median and inter-quartile range. The original data for DC gene expression are available at GEO repository (http://www.ncbi.nlm.nih.gov/geo/query/acc.cgi? acc=GSE32400) (B) Surface BST-2 expression (grey-filled histograms) relative to isotype control (black line histograms) for inactivated or R848-activated human CD14^{+} monocytes, CD16^{+} monocytes, BDCA-1 DCs, pDCs and Clec9A DCs. Data shown are representative of results for DCs isolated from seven human peripheral blood donors.

outcomes that resulted from delivering antigen to BST-2 expressed by defined DC subsets; steady state and activated pDCs, CD8^{+} DCs or CD8^{−} DCs. Both MHCI and MHCII antigen-presentation pathways were examined. To target antigen to BST-2, we utilised an antigen-delivery technique using an anti-biotin antibody conjugated to both OVA and FITC. Targeting BST-2 was compared to DEC205 [16] and Siglec-H [10, 17], two well-known receptors that have been targeted with antigen in previous studies.

First, the amount of antigen delivered to individual DC subsets by targeting BST-2, DEC205 or Siglec-H was determined (Fig. 3A). Steady state pDCs targeted via BST-2 received the highest antigen load, receiving almost sixfold higher levels of antibody-delivered OVA than either steady state or activated CD8^{+} or CD8^{−} DCs. Targeting BST-2 on pDCs, activated or steady state, resulted in a five to sixfold increase in delivered OVA relative to Siglec-H-targeted pDCs. There was no significant difference in antigen load delivered to BST-2-targeted cDCs, relative to DEC205-targeted cDCs. Differences in antigen presentation between BST-2, DEC205 and Siglec-H targeted DC subsets need to be considered in the context of this difference in the amount of antigen delivered.

Another determinant of antigen presentation is the kinetics of receptor endocytosis. To investigate this, we labeled DC subsets with biotinylated anti-BST-2, DEC205 or Siglec-H antibodies and assessed the presence of receptor remaining at the cell surface by staining with streptavidin-FITC after different culture periods. BST-2 is most rapidly internalised by steady state pDCs, compared with activated pDCs or activated cDCs. The levels of BST-2 on steady state cDCs were too low to perform analysis of endocy-

tosis. When compared with the internalisation of DEC205, activated cDCs endocytosed BST-2 more slowly. In contrast, BST-2 displayed faster internalisation kinetics than Siglec-H for both steady state and activated pDCs (Fig. 3B). Monitoring BST-2 trafficking in steady state pDCs showed internalised BST-2 accessed LAMP-1^{+} compartments (Fig. 3C).

MHCI and MHCII antigen presentation was assessed by incubating OVA-targeted DC subsets with OVA-specific OT-I and OT-II T cells, respectively. To determine the relative efficiency of different DC subsets to present antibody-delivered OVA, the maximum T-cell proliferation elicited by BST-2-OVA-targeted DC was compared. This was possible given that BST-2 is expressed by all of the DC subsets examined (Fig. 3D). For MHCI antigen presentation, activated CD8^{+} cDCs were the most efficient DC population at cross-presenting BST-2 targeted antigen, particularly relative to steady state pDCs that received the highest amount of BST-2-targeted antigen. In contrast, for MHCII antigen presentation, no specialization was observed with all of the BST-2-targeted DC subsets, both steady state and activated, eliciting similar MHCII antigen presentation capacity.

Antigen presentation of BST-2 versus DEC205 or Siglec-H-delivered antigen

To examine the efficiency of BST-2 as an antigen receptor, relative to other DC receptors, targeting of BST-2 versus DEC205 was compared. Steady state or activated CD8^{+} and CD8^{−} cDCs were
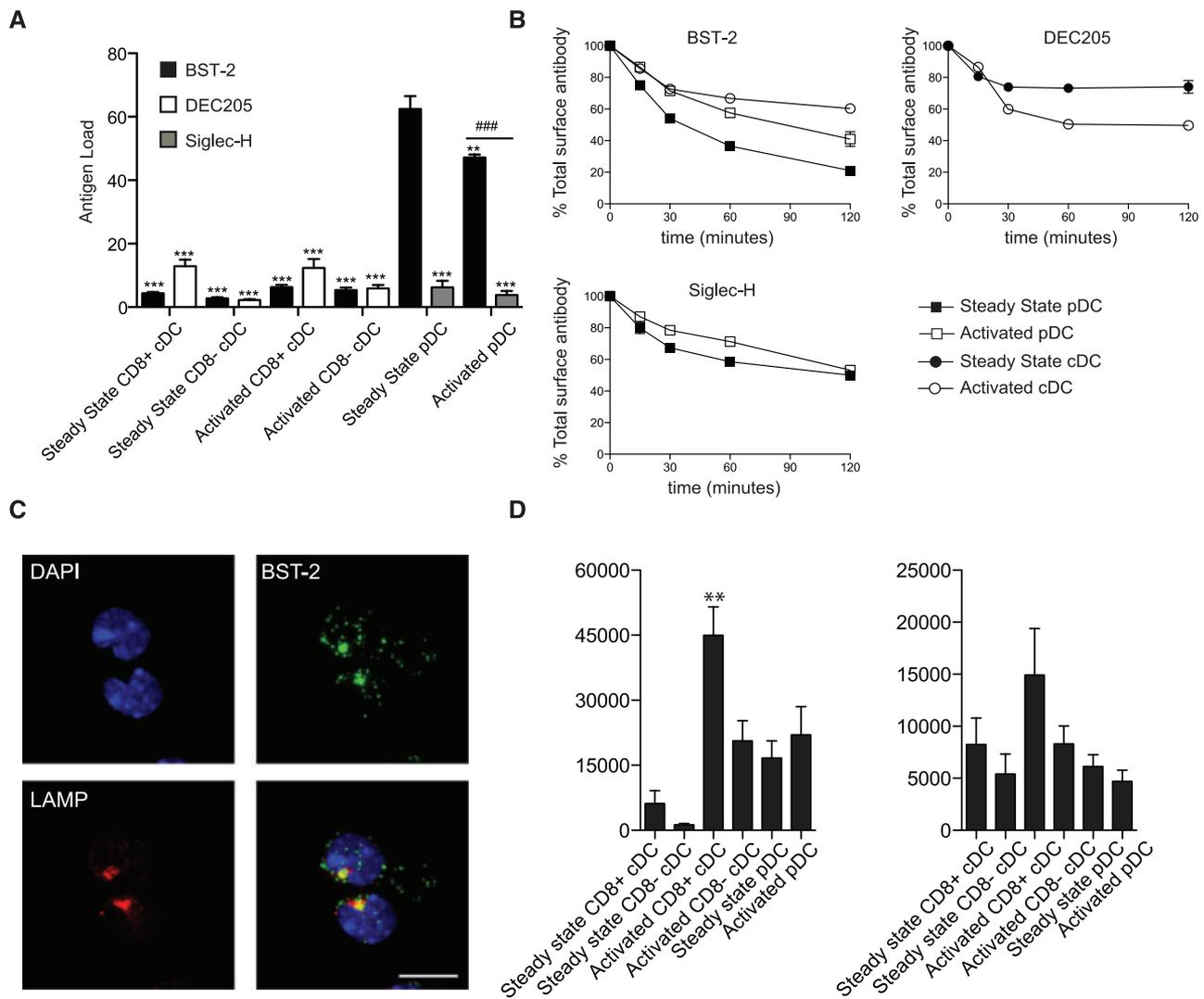
Figure 3. Antigen load, receptor internalisation and antigen presentation efficiency of targeted DC subsets. (A) DCs (steady state or in vivo activated) were labelled with biotinylated antibodies against BST-2, Siglec-H (pDCs) or DEC205 followed by anti-biotin antibodies conjugated to FITC and OVA protein. Antigen load is determined as a ratio of FITC mean fluorescence intensity compared to secondary antibody alone. The data are shown as mean + SEM of three to five mice pooled from three individual experiments. Data analysed by one-way ANOVA followed by Tukey's multiple comparison test. ***$p \leq 0.001$, relative to BST-2-targeted steady state pDCs, ### $p \leq 0.001$, relative to BST-2 targeted activated pDCs. (B) DCs were labelled with biotinylated anti-BST-2, DEC205 or Siglec-H antibodies, incubated at 37°C for various time points to allow internalisation of receptors. The amount of remaining surface protein was determined following surface staining with streptavidin-FITC. Data are shown as mean ± SEM of three individual samples and from one experiment that is representative of three independent experiments. (C) Sorted steady state pDCs were surface stained for BST-2 and incubated for 60 min to enable internalisation. Intracellular BST-2 localisation was determined by confocal microscopy. Scale bar is 10 μm. Data are representative of two independent experiments. (D) Sorted steady state pDCs, CD8$^+$ and CD8$^-$ cDCs and in vivo activated CD8$^+$, CD8$^-$ and pDC subsets were labeled with anti-BST-2-biotin followed by OVA-conjugated anti-biotin antibodies. DC subsets were co-cultured with CFSE-labelled OT-I or OT-II T cells for 64 h. Data are shown as mean + SEM of pooled data from three to seven individual experiments, performed in duplicate. $p \leq 0.0001$, one-way ANOVA followed by Tukey's multiple comparison test, relative to steady state pDCs, ** $p \leq 0.01$.

targeted with OVA delivered to BST-2 or DEC205. Titrated numbers of antigen targeted DCs were cultured with OVA-specific OT-I or OT-II T cells. Targeting either molecule expressed by steady state cDCs elicited poor MHCI or MHCII antigen-presentation outcomes, relative to targeting with secondary antibody alone, with no difference between BST-2 or DEC205 (Fig. 4A). In contrast, targeting activated CD8$^+$ and CD8$^-$ cDCs elicited robust OT-I and OT-II T-cell responses (Fig. 4B). In this case, targeting via BST-2

was less efficient than delivering OVA via DEC205 for MHCI, but not MHCII antigen presentation (Fig. 4B).

For pDCs, targeting efficiency for BST-2 was compared to Siglec-H. Steady state and activated pDCs were targeted with OVA delivered to BST-2 or Siglec-H (Fig. 4C). Titrated numbers of antigen targeted DCs were cultured with OVA-specific OT-I or OT-II T cells. Both MHCI and MHCII antigen presentation by pDCs in response to BST-2-targeted OVA elicited responses far superior
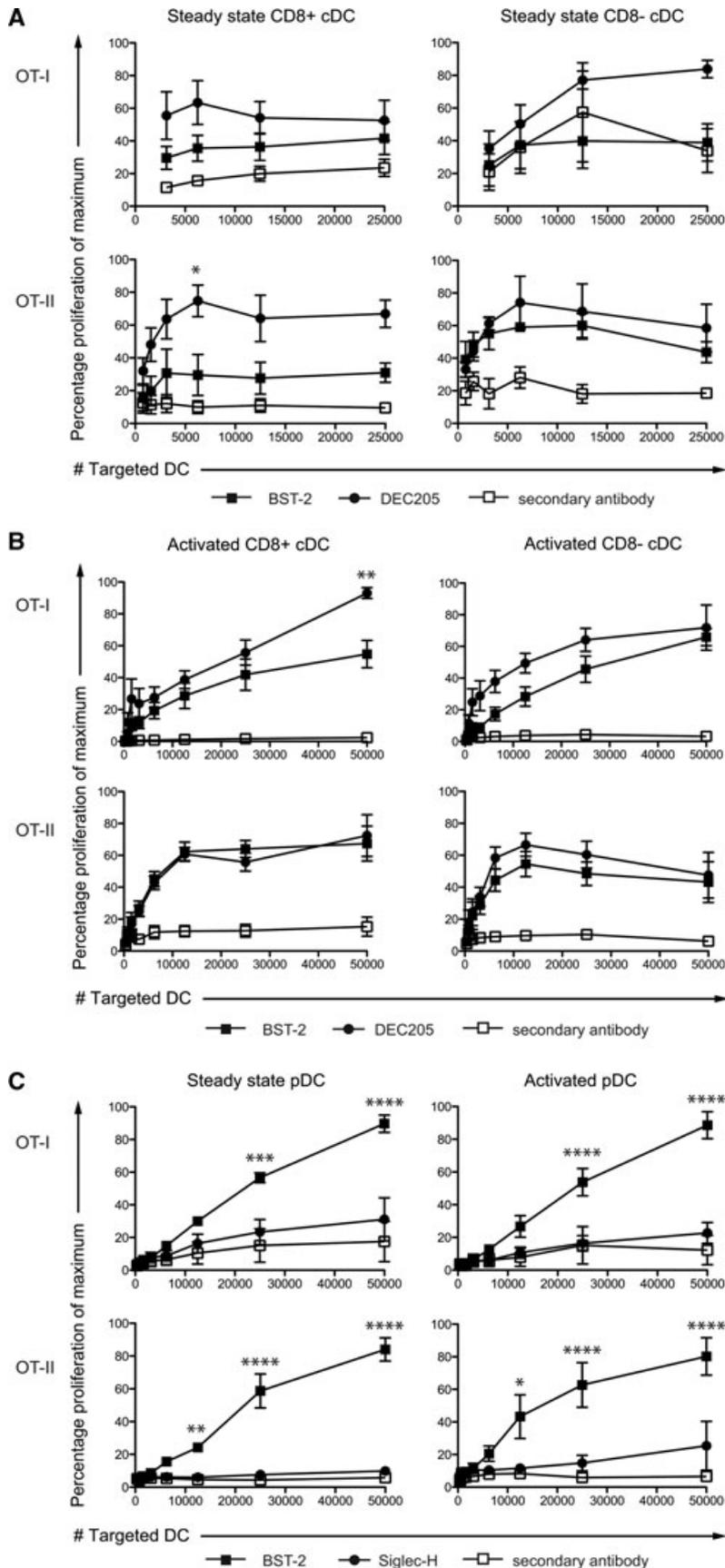
Figure 4. Antigen presentation of BST-2 versus DEC205 or Siglec-H-delivered antigen. (A) Steady state CD8$^+$ cDCs and CD8$^-$ cDCs or (B) in vivo activated CD8$^+$ cDCs and CD8$^-$ cDCs or (C) steady state or in vivo activated pDCs were labeled with biotinylated anti-BST-2, anti-DEC205 or anti-Siglec-H antibodies followed by OVA-conjugated anti-biotin antibodies. The DCs were titrated and co-cultured with CFSE-labelled OT-I or OT-II T cells for 64 h. Data are shown as the mean ± SEM of pooled data from seven individual experiments, performed in duplicate. Data analysed by two-way ANOVA, followed by Bonferroni multiple comparison, relative to BST-2 targeted cells, * $p \leq 0.05$, ** $p \leq 0.01$, *** $p \leq 0.001$, **** $p \leq 0.0001$.

to that elicited by Siglec-H-targeted OVA. Indeed, for MHCI, targeting Siglec-H failed to elicit OVA-specific responses above secondary control antibody alone, while for MHCII only very weak Siglec-H-mediated OVA presentation was observed (Fig. 4C).

In addition to targeting DCs in vitro, outcomes of targeting BST-2 in vivo were also assessed. To do this, anti-rat IgG antibody responses were measured 14 days after immunisation with 2 μg of rat anti-BST-2 antibody (120G8) or a rat isotype control antibody (GL113). Mice received anti-BST-2 antibody alone, anti-BST-2 antibody together with 20 nmol CpG or anti-BST-2 antibody 24 h after CpG treatment. In all cases, anti-BST-2 administered in vivo did not elicit anti-rat IgG responses (Supporting Information Fig. 1). This indicates that targeting BST-2 is inferior to targeting Clec9A [18] or Clec12A [19] that elicit anti-rat IgG responses by this protocol.

Discussion

Here we have examined targeting antigen via BST-2, a known receptor for the delivery of antigen in vivo [8–10]. We detect expression of BST-2 by several mouse and human DC subsets making it a useful receptor to target with antigen. We evaluated the outcomes of targeting BST-2-expressed by a panel of different DC subsets. Contrary to our proposal that BST-2 facilitates pDC antigen presentation, BST-2 targeted antigen was more efficiently presented by cDC. This occurs despite the high antigen load and efficient endocytosis following antigen delivery to BST-2 expressing pDC. While BST-2 is less efficient at eliciting MHCI cross-presentation relative to DEC205, BST-2 is a more efficient antigen delivery receptor than Siglec-H.

pDCs express high levels of *BST-2* mRNA and cell-surface protein, while other immune cell subsets increase *BST-2* transcription and surface expression following activation. The BST-2 surface protein expression pattern observed here is similar to that reported previously [1], while *BST-2* transcription had not previously been examined for a panel of immune cell subsets. In accordance with previous reports [1,20], BST-2 exhibits a promiscuous expression pattern following activation, with expression up-regulated at the surface of all immune subsets examined. We observed expression at high levels by both major DC populations at sites of live viral infection. *BST-2* is an IFN responsive gene [1, 20, 21] with its promoter containing an IFN regulatory factor binding site [22], together with response elements for several inflammatory cytokines [23] that are likely to mediate the increase in *BST-2* expression observed following in vitro and in vivo activation. Notably, surface BST-2 levels differ between mouse and human pDCs. As we have shown here and supported by other studies, human blood pDCs express low or no BST-2, but upregulate its expression after activation [3, 15]. Interestingly, we detect high BST-2 expression by two major human myeloid DC subsets; BDCA1 and Clec9A DCs. This has not previously been examined and serves to highlight the importance of targeting antigen to BST-2 expressed by DC subsets other than pDCs. This is important if this strategy is to be translated into clinical settings.

Given the broad expression pattern of BST-2 by various DC subsets following activation, we assessed whether purified CD8+ and CD8− cDC subsets present BST-2-targeted antigen. Both MHCI and MHCII antigen presentation by BST-2-targeted activated CD8+ and CD8− cDCs was observed. Targeting BST-2 expressed by a panel of DC subsets enabled us to undertake a direct comparison of the antigen-presentation efficiency of different DCs. This has not been undertaken previously, as previous in vivo targeting with BST-2 was performed under conditions where BST-2 was not expressed by cDCs [8–10]. Despite large differences in antigen load, for cross-presentation via MHCI, CD8+ DCs were superior to the other DC subsets analysed. This is in accordance with the known role for CD8+ DCs as the major cross-presenting DC subset [24, 25]. Delivering antigen via DEC205 elicited more efficient cross-presentation than BST-2, which indicates a more efficient ability of this receptor to access the cross-presentation compartment. Activated CD8− DCs and pDCs were also capable of cross-presenting antibody-targeted antigen, although at a lower efficiency than CD8+ DCs. This has been previously described for DEC205 [16] and BST-2 [9]-targeted antigen. Notably, activation of CD8+ and CD8− DCs did not impair their ability to present targeted antigen, unlike soluble protein or cell-associated antigen that cannot be presented by activated DCs [26]. This agrees with previous reports where antibody-mediated delivery of OVA to DEC205 elicited MHCII antigen presentation by activated DCs [27, 28]. Therefore, while activated DCs shut down macropinocytosis and phagocytosis, they retain the capacity to undertake receptor-mediated endocytosis. This is a useful attribute to exploit when targeting antigen to DCs in immunisation settings. Finally, our data suggest that pDCs, even following activation, are inferior antigen-presenting cells when compared to cDCs for receptor-targeted antigen. Despite receiving approximately sixfold higher amounts of antigen than their cDC counterparts, steady state and activated pDCs elicited inferior MHCI cross-presentation and did not promote enhanced MHCII responses compared with that elicited by cDC subsets receiving significantly less antigen. This concurs with previous reports, where pDCs are less efficient presenters than cDCs, of soluble OVA protein [7, 29]. Given the reduced antigen-presentation efficiency with which pDCs present BST-2-targeted OVA relative to BST-2 targeted to cDCs, we would expect cDCs to contribute to BST-2-mediated immunity in vivo. Therefore, to ensure robust immunity is elicited by DC targeting strategies, utilising receptors that are preferentially expressed by cDCs, rather than pDCs, would be the more advantageous strategy.

Targeting antigen to BST-2 was compared to two well-known DC surface markers, DEC205 and Siglec-H. DEC205 has pioneered studies of antigen targeting to DC receptors. It is expressed by cDCs and elicits robust T-cell immunity when targeted with antigen [16]. Studies targeting antigen to DEC205 have pioneered the development of T-cell based vaccines for HIV [30]. Siglec-H, unlike DEC205, is not expressed by cDCs but is restricted to pDCs. Targeting antigen to Siglec-H is capable of initiating CD4+ T-cell responses, although the cells that develop are ultimately hypo-responsive [10], and can elicit CD8+ T-cell immune responses in vivo [17]. Relative to DEC205, BST-2 was the inferior

receptor to target on activated cDCs in order to initiate MHCI antigen presentation. In contrast, for MHCII antigen presentation BST-2 and DEC205 were mostly comparable. BST-2 was a far superior target receptor, relative to Siglec-H, when delivering antigen to steady state or activated pDCs for MHCI or MHCII antigen presentation.

In summary, several mechanisms contribute to successful outcomes for targeting specific DC molecules including the specific DC subset targeted, the kinetics of receptor internalisation and the delivered antigen load. Here, we have defined these for BST-2, an interesting molecule that is already the focus of antigen targeting strategies. In-depth understanding of the parameters of antigen targeting is required if this strategy is to be successfully applied to clinical settings.

Materials and methods

Mice

C57BL/6, OT-I [31] and OT-II [32] mice were bred under specific pathogen-free conditions at the Walter and Eliza Hall Institute. Gender- and age-matched (6–12 weeks) animals were used. For activation of immune cells by CpG, mice were injected intravenously with fully phosphorothioated 20 nmol CpG 1668, type B (Geneworks) 24 h prior to organ harvest. Mice were infected with 1×10^4 PFU of HKx31 influenza A virus. All experiments were conducted in accordance with guidelines provided by National Health and Medical Research Council of Australia. Experimental procedures were approved by the Animal Ethics Committee, Melbourne Health Research Directorate.

Isolation of mouse immune cells

DCs were isolated from the spleen or lung. Organs were digested with 140 μg/mL DNAse (Roche Applied Science) and 1 mg/mL collagenase type 3 (Worthington Biochemicals) and intercellular clusters disrupted by 0.01M EDTA treatment. Low-density cells were isolated by density centrifugation (1.077 g/cm³ Nycodenz). DC was enriched by magnetic depletion of unwanted cells using a cocktail of rat anti-mouse antibodies (KT3–1.1, anti-CD3; T24/31.7, anti-Thy1; TER119, anti-erythrocytes; RA36B2, anti-CD45R or 1D3 anti-CD19; RB6–8C5, anti-Ly6C/G or 1A8, Ly6G) and magnetic beads conjugated to anti-rat antibodies (Qiagen Biomags). DC isolation yielded cell preparations with approximately 70–85% CD11c⁺ purity.

Lymphocytes were isolated from spleen and LN. OT-I and OT-II T cells were isolated from LNs and enriched by magnetic depletion of unwanted cells using a cocktail of rat anti-mouse antibodies T24/31.7, anti-CD90; RB6-8C5, anti-Gr-1; anti-B220 (RA3–6B2), anti-erythrocyte (Ter-119)) and magnetic beads conjugated

to anti-rat antibodies (Qiagen Biomags). Macrophages were isolated from the peritoneal cavity of mice using 10 mL PBS washes.

Cells were identified for flow cytometry using the following markers (antibody clones); cDC: CD11c (N418), CD8 (YTS169), pDC; Ly6c (5075–3.6) and/or CD45RA (14.8), B cells; CD19 (1D3) or B220 (RA36B2), T cells: CD3 (KT3–1.1), CD4 (GK1.5), CD8 (YTS169), macrophages; CD11b (M1/70), F4/80 (F4/80). BST-2 was identified using the rat anti-mouse antibody 120.G8 compared to isotype control IgG1κ. All antibodies were generated in house, except the isotype control (Biolegend). Samples were analysed using an FACS Calibur or LSR2 (BD Biosciences) and sorted using a Moflo (Dake Cytomation) or FACSAria (BD Biosciences). Refer to Supporting Information Fig. 2 for flow cytometry gating strategy.

For activation in vitro, all cells were cultured in RPMI 1640 medium containing 10% FCS, 100 U/mL penicillin and 100 μg/mL streptomycin, 10^{-4} M 2-mercaptoethanol at 37°C, 10% CO₂. DC was cultured for 24 h in media supplemented with 10 ng/mL GM-CSF and 0.5 nmol/mL CpG (1668, type B). Peritoneal macrophages were cultured with 100 ng/mL of IFN-γ for 8 h, followed by 16-h incubation in media containing 1 μg/mL LPS. B cells were cultured for 24 h in media containing 50 μg/mL of anti-CD40 antibody (clone FGK45.5). T cells were cultured for 48 h in the presence of 5 μg/ml anti-CD28 antibody (clone 37.51), 10 U/mL IL-2 and plate-bound anti-CD3 antibody (clone 145.2CII).

Quantitative realtime PCR

RNA was isolated from sorted cell populations (Qiagen RNeasy Plus kit). A total of 100 ng of RNA was used to generate cDNA (Qiagen QuantiTec RT PCR kit). SYBR green master mix (Roche) was used in quantitative PCR reactions on the Lightcycler 480 (Roche). BST-2 mRNA expression was normalised to housekeeping gene transferin receptor 2. BST-2 mRNA was identified by forward 5′ATGGCGCCCTCTTTCTATCAC3′ and reverse 5′GTCTCTACAGGCCACGCTGTTC3′ primers. Gene transferin receptor 2 mRNA was identified by forward 5′ TATCGGCTGGGACCTGGGCC 3′ and reverse 5′GCTCCTGGGCCCCATGCATC3′ primers.

Isolation of human immune cells

Peripheral blood mononuclear cells (PBMCs) were isolated from seronegative healthy donors provided by the Australian Red Cross Bank. Monocyte-derived DCs were differentiated from CD14⁺ monocytes by culture in IL-4 and GM-CSF to generate immature monocyte-derived DCs as previously described [33, 34]. Mature monocyte-derived DCs were generated following culture in the presence of TNF-α. Total blood DCs and monocytes were enriched from PBMCs using magnetic bead depletion (MiltenyiBiotec) as previously described [35]. DCs were further sorted into myeloid

(HLA-DR$^+$ CD11c$^+$) and plamacytoid (HLA-DR$^+$ CD123$^+$) subsets using flow cytometry. Isolation of skin DC subsets (CD14 dermal DCs, CD1a dermal DCs and Langerhans cells) was performed as previously described [36]. Human CD34$^+$ acute myeloid leukemia MUTZ3 cells were provided by S. Santegoets from VU University Medical Center, Netherlands [37]. Resting CD4$^+$ T cells were purified as previously described [38]. Purified T cells were cultured alone, with CCL19 or PHA and IL-2.

For human monocyte and DC analysis, buffy coats from healthy donors were obtained from Etablissement Français du Sang. PBMCs were prepared by centrifugation on a Ficoll gradient (Lymphoprep, Greiner Bio-One). PBMCs were either analysed after isolation or after overnight culture in RPMI-Glutamax medium (Gibco) containing 10% FCS and 1 μg/mL of R848 (Invitrogen). Cells were stained with anti-CD16 (BD Biosciences), anti-BDCA4 (Miltenyi Biotec), anti-BDCA-1 (eBioscience), anti-CD4 (BD Biosciences), anti-CD14 (Miltenyi Biotec), anti-Clec9A (Miltenyi Biotec), anti-BST2 (Biolegend) or isotype-matched control antibody. Cell viability was assessed with DAPI. Cells were analysed on an FACSVerse (BD Biosciences) instrument. Data were analysed with FlowJo (Tree Star).

Microarray hybridisation and data analysis

Total RNA was extracted from purified cell populations from individual donors and processed for hybridisation to 1 of 55 cDNA gene arrays (Human ResGen 8k, Australian Genome Research Facility, Melbourne, Australia) using a common monocyte-derived DC reference, or 24 bead arrays (sentrix human 6 v2 expression chips), Illumina, San Diego, CA). The RNA extraction, labelling, hybridisation, data processing and analysis procedures are described previously for the cDNA gene array and Illumina arrays, respectively [33, 39]. Clustered data were further processed in PARTEK Genomics Suite (Partek Inc., St. Lois, MO, USA) to exclude genes not showing detectable expression in more than 80% of arrays and to remove batch effects. Microarray data is available through the Gene Expression Omnibus database (http://www.ncbi.nlm.nih.gov/geo/).

Microscopy

Steady state pDCs were stained with biotin-BST-2 and streptavidin-Alexa 488 (Invitrogen, Molecular Probes) at 4°C and then incubated at 37°C for 60 min. Cells were attached to cover slips with anti-MHCI antibody (Y3) for 10 min at room temperature. Cover slips were washed in PBS, samples were fixed in 4% PFA (Sigma Aldrich) and permabilised with 0.3% Triton X 100 (Sigma Aldrich) prior to staining for LAMP-1 (Abcam). Nuclei were stained with 5 μg/mL DAPI (Invitrogen). Cover slips were mounted with DAKO mounting media. Images were acquired on an LSM700 confocal microscope (Zeiss) and analysed with ImageJ software.

Antigen-presentation assay

Sorted pDC and CD8$^+$ or CD8$^-$ cDC were labelled with anti-BST-2 biotin (clone 120.G8), anti-DEC205-biotin (clone NLDC145) or anti-Siglec-H-biotin (clone 551.3D3) on ice for 30 min, washed twice and labelled with anti-biotin OVA (Miltenyi Biotec) for 15 min at 4°C. Cells were then washed twice and re-suspended in culture media containing CpG (1688, type B) and 10 ng/mL GM-CSF, titrated and incubated with CFSE-labelled OT-I or OT-II transgenic T cells for 64 h. Dividing cells were determined as T cells that had diluted the CFSE dye by flow cytometry. Refer to Supporting Information Fig. 3 for flow cytometry gating strategy.

Internalisation assay

Cells were stained either with biotinylated anti-BST-2 (clone 120.G8), anti-DEC205 (clone NLDC145) or anti-Siglec-H (clone 551.3D3) antibodies on ice for 30 min, washed twice and incubated for various time periods at 37°C allowing the BST-2 antibody to be internalised. Cells were then stained for surface markers and streptavidin-FITC and analysed on the LSR II (Becton Dickinson).

References

1 Blasius, A. L., Giurisato, E., Cella, M., Schreiber, R. D., Shaw, A. S. and Colonna, M., Bone marrow stromal cell antigen 2 is a specific marker of type I IFN-producing cells in the naive mouse, but a promiscuous cell surface antigen following IFN stimulation. *J. Immunol.* 2006. **177:** 3260–3265.

2 Swiecki, M., Scheaffer, S. M., Allaire, M., Fremont, D. H., Colonna, M. and Brett, T. J., Structural and biophysical analysis of BST-2/tetherin ectodomains reveals an evolutionary conserved design to inhibit virus release. *J. Biol. Chem.* 2011. **286:** 2987–2997.

3 Cao, W., Bover, L., Cho, M., Wen, X., Hanabuchi, S., Bao, M., Rosen, D. B. et al., Regulation of TLR7/9 responses in plasmacytoid dendritic cells by BST2 and ILT7 receptor interaction. *J. Exp. Med.* 2009. **206:** 1603–1614.

4 **Neil, S. J., Zang, T. and Bieniasz, P. D.**, Tetherin inhibits retrovirus release and is antagonized by HIV-1 Vpu. *Nature* 2008. **451:** 425–430.

5 **Evans, D. T., Serra-Moreno, R., Singh, R. K. and Guatelli, J. C.**, BST-2/tetherin: a new component of the innate immune response to enveloped viruses. *Trends Microbiol.* 2010. **18:** 388–396.

6 **Villadangos, J. A. and Young, L.**, Antigen-presentation properties of plasmacytoid dendritic cells. *Immunity* 2008. **29:** 352–361.

7 **Kool, M., Geurtsvankessel, C., Muskens, F., Madeira, F. B., van Nimwegen, M., Kuipers, H., Thielemans, K. et al.**, Facilitated antigen uptake and timed exposure to TLR ligands dictate the antigen-presenting potential of plasmacytoid DCs. *J. Leukoc. Biol.* 2011. **90:** 1177–1190.

8 **Sapoznikov, A., Fischer, J. A., Zaft, T., Krauthgamer, R., Dzionek, A. and Jung, S.**, Organ-dependent in vivo priming of naive CD4+, but not CD8+, T cells by plasmacytoid dendritic cells. *J. Exp. Med.* 2007. **204:** 1923–1933.

9 **Loschko, J., Schlitzer, A., Dudziak, D., Drexler, I., Sandholzer, N., Bourquin, C., Reindl, W. et al.**, Antigen delivery to plasmacytoid dendritic cells via BST2 induces protective T-cell-mediated immunity. *J. Immunol.* 2011. **186:** 6718–6725.

10 **Loschko, J., Heink, S., Hackl, D., Dudziak, D., Reindl, W., Korn, T. and Krug, A. B.**, Antigen targeting to plasmacytoid dendritic cells via Siglec-H inhibits Th cell-dependent autoimmunity. *J. Immunol.* 2011. **187:** 6346–6356.

11 **Swiecki, M., Wang, Y., Gilfillan, S., Lenschow, D. J. and Colonna, M.**, Cutting edge: paradoxical roles of BST2/tetherin in promoting type I IFN response and viral infection. *J. Immunol.* 2012. **188:** 2488–2492.

12 **Caminschi, I., Lahoud, M. H. and Shortman, K.**, Enhancing immune responses by targeting antigen to DC. *Eur. J. Immunol.* 2009. **39:** 931–938.

13 **Chiriva-Internati, M., Liu, Y., Weidanz, J. A., Grizzi, F., You, H., Zhou, W., Bumm, K. et al.**, Testing recombinant adeno-associated virus-gene loading of dendritic cells for generating potent cytotoxic T lymphocytes against a prototype self-antigen, multiple myeloma HM1.24. *Blood* 2003. **102:** 3100–3107.

14 **Jalili, A., Ozaki, S., Hara, T., Shibata, H., Hashimoto, T., Abe, M., Nishioka, Y. et al.**, Induction of HM1.24 peptide-specific cytotoxic T lymphocytes by using peripheral-blood stem-cell harvests in patients with multiple myeloma. *Blood* 2005. **106:** 3538–3545.

15 **Erikson, E., Adam, T., Schmidt, S., Lehmann-Koch, J., Over, B., Goffinet, C., Harter, C. et al.**, In vivo expression profile of the antiviral restriction factor and tumor-targeting antigen CD317/BST-2/HM1.24/tetherin in humans. *Proc. Natl. Acad. Sci. USA* 2011. **108:** 13688–13693.

16 **Dudziak, D., Kamphorst, A. O., Heidkamp, G. F., Buchholz, V. R., Trumpfheller, C., Yamazaki, S., Cheong, C. et al.**, Differential antigen processing by dendritic cell subsets in vivo. *Science* 2007. **315:** 107–111.

17 **Zhang, J., Raper, A., Sugita, N., Hingorani, R., Salio, M., Palmowski, M. J., Cerundolo, V. et al.**, Characterization of Siglec-H as a novel endocytic receptor expressed on murine plasmacytoid dendritic cell precursors. *Blood* 2006. **107:** 3600–3608.

18 **Caminschi, I., Proietto, A. I., Ahmet, F., Kitsoulis, S., Shin Teh, J., Lo, J. C., Rizzitelli, A. et al.**, The dendritic cell subtype-restricted C-type lectin Clec9A is a target for vaccine enhancement. *Blood* 2008. **112:** 3264–3273.

19 **Lahoud, M. H., Proietto, A. I., Ahmet, F., Kitsoulis, S., Eidsmo, L., Wu, L., Sathe, P. et al.**, The C-type lectin Clec12A present on mouse and human dendritic cells can serve as a target for antigen delivery and enhancement of antibody responses. *J. Immunol.* 2009. **182:** 7587–7594.

20 **Liberatore, R. A. and Bieniasz, P. D.**, Tetherin is a key effector of the antiretroviral activity of type I interferon in vitro and in vivo. *Proc. Natl. Acad. Sci. USA* 2011. **108:** 18097–18101.

21 **Kawai, S., Azuma, Y., Fujii, E., Furugaki, K., Ozaki, S., Matsumoto, T., Kosaka, M. et al.**, Interferon-alpha enhances CD317 expression and the antitumor activity of anti-CD317 monoclonal antibody in renal cell carcinoma xenograft models. *Cancer Sci.* 2008. **99:** 2461–2466.

22 **Bego, M. G., Mercier, J. and Cohen, E. A.**, Virus-activated interferon regulatory factor 7 upregulates expression of the interferon-regulated BST2 gene independently of interferon signaling. *J. Virol.* 2012. **86:** 3513–3527.

23 **Ohtomo, T., Sugamata, Y., Ozaki, Y., Ono, K., Yoshimura, Y., Kawai, S., Koishihara, Y. et al.**, Molecular cloning and characterization of a surface antigen preferentially overexpressed on multiple myeloma cells. *Biochem. Biophys. Res. Commun.* 1999. **258:** 583–591.

24 **den Haan, J. M., Lehar, S. M. and Bevan, M. J.**, CD8(+) but not CD8(-) dendritic cells cross-prime cytotoxic T cells in vivo. *J. Exp. Med.* 2000. **192:** 1685–1696.

25 **Schnorrer, P., Behrens, G. M., Wilson, N. S., Pooley, J. L., Smith, C. M., El-Sukkari, D., Davey, G. et al.**, The dominant role of CD8+ dendritic cells in cross-presentation is not dictated by antigen capture. *Proc. Natl. Acad. Sci. USA* 2006. **103:** 10729–10734.

26 **Wilson, N. S., Behrens, G. M., Lundie, R. J., Smith, C. M., Waithman, J., Young, L., Forehan, S. P. et al.**, Systemic activation of dendritic cells by Toll-like receptor ligands or malaria infection impairs cross-presentation and antiviral immunity. *Nat. Immunol.* 2006. **7:** 165–172.

27 **Platt, C. D., Ma, J. K., Chalouni, C., Ebersold, M., Bou-Reslan, H., Carano, R. A., Mellman, I. et al.**, Mature dendritic cells use endocytic receptors to capture and present antigens. *Proc. Natl. Acad. Sci. USA* 2010. **107:** 4287–4292.

28 **Kamphorst, A. O., Guermonprez, P., Dudziak, D. and Nussenzweig, M. C.**, Route of antigen uptake differentially impacts presentation by dendritic cells and activated monocytes. *J. Immunol.* 2010. **185:** 3426–3435.

29 **Young, L. J., Wilson, N. S., Schnorrer, P., Proietto, A., ten Broeke, T., Matsuki, Y., Mount, A. M. et al.**, Differential MHC class II synthesis and ubiquitination confers distinct antigen-presenting properties on conventional and plasmacytoid dendritic cells. *Nat. Immunol.* 2008. **9:** 1244–1252.

30 **Cheong, C., Choi, J. H., Vitale, L., He, L. Z., Trumpfheller, C., Bozzacco, L., Do, Y. et al.**, Improved cellular and humoral immune responses in vivo following targeting of HIV Gag to dendritic cells within human anti-human DEC205 monoclonal antibody. *Blood* 2010. **116:** 3828–3838.

31 **Clarke, S. M. R., Barnden, M., Kurts, C., Carbone, F. R., Miller, J. F. A. P. and Heath, W. R.**, Characterisation of the OVA-specific TCR transgenic line OT-I: MHC elements for positive and negative selection. *Immunol. Cell Biol.* 2000. **78:** 110–117.

32 **Barnden, M. J., Allison, J., Heath, W. R. and Carbone, F. R.**, Defective TCR expression in transgenic mice constructed using cDNA-based alpha- and beta-chain genes under the control of heterologous regulatory elements. *Immunol. Cell Biol.* 1998. **76:** 34–40.

33 **Harman, A. N., Wilkinson, J., Bye, C. R., Bosnjak, L., Stern, J. L., Nicholle, M., Lai, J. et al.**, HIV induces maturation of monocyte-derived dendritic cells and Langerhans cells. *J. Immunol.* 2006. **177:** 7103–7113.

34 **Turville, S. G., Santos, J. J., Frank, I., Cameron, P. U., Wilkinson, J., Miranda-Saksena, M., Dable, J. et al.**, Immunodeficiency virus uptake, turnover, and 2-phase transfer in human dendritic cells. *Blood* 2004. **103:** 2170–2179.

35 **Cameron, P. U., Handley, A. J., Baylis, D. C., Solomon, A. E., Bernard, N., Purcell, D. F. and Lewin, S. R.**, Preferential infection of dendritic cells during human immunodeficiency virus type 1 infection of blood leukocytes. *J. Virol.* 2007. **81:** 2297–2306.

36 **McLellan, A. D., Heiser, A., Sorg, R. V., Fearnley, D. B. and Hart, D. N.**, Dermal dendritic cells associated with T lymphocytes in normal human skin display an activated phenotype. *J. Invest. Dermatol.* 1998. **111:** 841–849.

37 **de Jong, M. A., de Witte, L., Santegoets, S. J., Fluitsma, D., Taylor, M. E., de Gruijl, T. D. and Geijtenbeek, T. B.**, Mutz-3-derived Langerhans cells are a model to study HIV-1 transmission and potential inhibitors. *J. Leukoc. Biol.* 2010. **87:** 637–643.

38 **Saleh, S., Solomon, A., Wightman, F., Xhilaga, M., Cameron, P. U. and Lewin, S. R.**, CCR7 ligands CCL19 and CCL21 increase permissiveness of resting memory CD4^{+} T cells to HIV-1 infection: a novel model of HIV-1 latency. *Blood* 2007. **110:** 4161–4164.

39 **Harman, A. N., Kraus, M., Bye, C. R., Byth, K., Turville, S. G., Tang, O., Mercier, S. K. et al.**, HIV-1-infected dendritic cells show 2 phases of gene expression changes, with lysosomal enzyme activity decreased during the second phase. *Blood* 2009. **114:** 85–94.

Full correspondence: Dr. Justine D. Mintern, The University of Melbourne, Bio21, 30 Flemington Rd, Parkville Victoria 3010, Australia
Fax: +61-3-9348-1421
e-mail: jmintern@unimelb.edu.au

Additional correspondence: Prof. Jose A. Villadangos, The University of Melbourne, Bio21, 30 Flemington Rd, Parkville Victoria 3010, Australia
Fax: +61-3-9348-1421
e-mail: j.villadangos@unimelb.edu.au